Entropy **2014**, *16*, 3710-3731; doi:10.3390/e16073710

OPEN ACCESS

entropy

ISSN 1099-4300

www.mdpi.com/journal/entropy

Article

The Role of Vegetation on the Ecosystem Radiative Entropy Budget and Trends Along Ecological Succession

Paul C. Stoy [1,*], Hua Lin [2], Kimberly A. Novick [3], Mario B. S. Siqueira [4] and Jehn-Yih Juang [5]

[1] Department of Land Resources and Environmental Sciences, Montana State University, Bozeman, MT 59717, USA

[2] Key Laboratory of Tropical Forest Ecology, Xishuangbanna Tropical Botanical Garden, Chinese Academy of Sciences, Mengla, Yunnan, 666303, China; E-Mail: lh@xtbg.ac.cn

[3] School of Public and Environmental Affairs, Indiana University—Bloomington, 702 N Walnut Grove Ave., Bloomington, IN 47405, USA; E-Mail: knovick@indiana.edu

[4] Department of Mechanical Engineering, University of Brasilia, Brasilia 70910-900, Brazil; E-Mail: mariosiqueira@unb.br

[5] Department of Geography, National Taiwan University, Taipei 10617, Taiwan; E-Mail: jjuang@ntu.edu.tw

* Author to whom correspondence should be addressed; E-Mail: paul.stoy@montana.edu; Tel.: +1-406-994-5927; Fax: +1-406-994-3933.

Received: 1 March 2014; in revised form: 6 June 2014 / Accepted: 12 June 2014 / Published: 3 July 2014

Abstract: Ecosystem entropy production is predicted to increase along ecological succession and approach a state of maximum entropy production, but few studies have bridged the gap between theory and data. Here, we explore radiative entropy production in terrestrial ecosystems using measurements from 64 Free/Fair-Use sites in the FLUXNET database, including a successional chronosequence in the Duke Forest in the southeastern United States. Ecosystem radiative entropy production increased then decreased as succession progressed in the Duke Forest ecosystems, and did not exceed 95% of the calculated empirical maximum entropy production in the FLUXNET study sites. Forest vegetation, especially evergreen needleleaf forests characterized by low shortwave albedo and close coupling to the atmosphere, had a significantly higher ratio of radiative entropy production to the empirical maximum entropy production than did croplands and grasslands. Our results demonstrate that ecosystems approach, but do not reach, maximum entropy production and that the relationship between succession and entropy production depends on vegetation characteristics. Future studies should investigate how natural

disturbances and anthropogenic management—especially the tendency to shift vegetation to an earlier successional state—alter energy flux and entropy production at the surface-atmosphere interface.

Keywords: climate zone; ecosystem energy balance; entropy; plant functional type; radiometric surface temperature

1. Introduction

Organisms dissipate energy to maintain a state that is far from thermodynamic equilibrium [1,2]. Beginning with Lotka [3], research has focused on how organisms capture energy more efficiently to gain a competitive advantage in the struggle for existence. An outcome of this line of reasoning is that ecosystem energy flux should increase with ecological succession as these "suitably constituted organisms" that comprise a developed ecosystem "enlarge the total energy flux" [3]. As a consequence, multiple theoretical and empirical investigations have argued that entropy production should increase with ecosystem succession (e.g., [2,4,5]) following the Maximum Entropy Production Principle (MEPP): non-equilibrium thermodynamic systems are organized in steady state such that the rate of entropy production is maximized [6]. Few have used observations to document these predicted changes in terrestrial ecosystems [7–9], although numerous studies have demonstrated the applicability of MEPP to aquatic ecosystems [10–14] and metabolic networks [15].

Other studies, ultimately following the work of Jaynes [16], take a statistical viewpoint and argue that a state of maximum entropy production is the most likely state of an ecosystem as it develops new pathways to dissipate energy [17–19]. Empirical confirmations of this prediction once more are few [7]. Do ecosystems reach a state of maximum entropy production as they develop? If not, why?

Holdaway *et al.* [7] proposed a general model of ecosystem entropy changes along succession in which ecosystem entropy production, σ, increases with ecosystem development, approaches a state of maximum entropy production, and declines slightly with ecosystem retrogression, Observations from different tropical vegetation types provided initial support for their conceptual model (see Figure 5 in [7]). It remains unclear if ecosystem entropy production reaches a maximum value and thereby a steady state following the MEPP, how close different ecosystem types come to a state of maximum entropy production, and if entropy production follows the proposed pattern of growth/maturation/regression as predicted by ecological theories like the Strategy of Ecosystem Development [20] that motivated the model. Skene [5] derived a logistic model for entropy production along succession that follows the MEPP, which suggests that ecosystem entropy increases along succession then approaches an asymptote of approximately 0.5 W m^{-2} K^{-1} following observations from Holdaway *et al.* [7]. Again these theoretical predictions have yet to be tested using observations.

As we will show in the next section, the imbalance between actual and maximum entropy production is linked to a number of ecosystem physiological and structural properties, including energy capture via the shortwave albedo and the canopy properties the control the surface conductance and thus the coupling between surface and air temperature. With these considerations, and following Odum [20], we hypothesize that σ will increase then decrease along a successional trajectory due to an

increase then decrease in solar energy capture (*i.e.*, albedo), but that ecosystems do not reach a state of maximum entropy production regardless of successional stage because they cannot capture and dissipate all available energy. We test these hypotheses using radiometric and micrometeorological measurements from the Duke Forest, NC, USA and develop an empirical approach for estimating maximum entropy production, which we term "empirical maximum entropy production" (EMEP). We further hypothesize that forest vegetation, which is characteristic of the middle to late stages of succession, will have greater σ than short-statured vegetation like grasslands when normalized for EMEP. We test this hypothesis using observations from 64 ecosystems from the Free/Fair Use FLUXNET database and further explore if the proposed value 0.5 W m^{-2} K^{-1} is a good approximation of maximum radiative entropy production in terrestrial ecosystems [5,7].

2. Theory and Methods

We first discuss measurements to calculate σ and an approach to estimate the empirical maximum entropy production (EMEP) of an ecosystem under typical conditions. We then describe the eddy covariance and micrometeorological measurements used to calculate σ and EMEP across different ecosystem and climate types and the statistical analyses used to ascertain if the ratio of σ to EMEP differs among climate and vegetation types, and along ecological succession.

2.1. Ecosystem Energy Balance

Any study of σ must begin with the ecosystem energy balance, in which the net radiation (R_n) equals incident shortwave radiation ($Q_{S,in}$) minus outgoing shortwave radiation ($Q_{S,out}$) plus incident longwave radiation ($Q_{L,in}$) minus outgoing longwave radiation ($Q_{L,out}$) (Figure 1).

Figure 1. Energy flux (Q) and entropy production (σ) at the terrestrial ecosystem-atmosphere interface including incident solar radiation and reflected shortwave radiation (the difference between which is net shortwave radiation, $Q_{S,net}$) and the associated entropy production term (σ_{QS}), net longwave radiation ($Q_{L,net}$) and associated entropy production (σ_{QL}). The present study concerns entropy production owing to the terms within the dashed box. Entropy production arising from latent heat (LE), sensible heat (H), and ecosystem metabolism (M) are excluded.

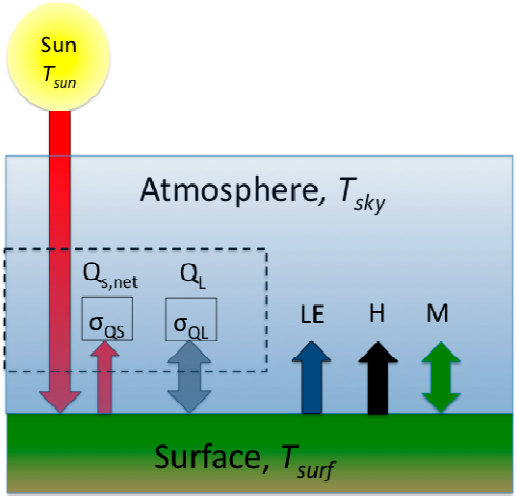

R_n is dissipated by latent heat flux (*LE*, *i.e.*, evapotranspiration), sensible heat flux (*H*, *i.e.*, thermals), ecosystem heat flux (*G*, often assumed to equal soil heat flux), and any net energy flux *M* owing to carbon fixation and the growth, maintenance, and reproductive sources of ecosystem respiration [15]:

$$R_n = Q_{S,in} - Q_{S,out} + Q_{L,in} - Q_{L,out} = LE + H + G + M \quad (1)$$

2.2. Ecosystem Entropy Production (σ)

We calculate σ following Brunsell *et al.* [21], noting also the approach of Holdaway *et al.* [7]. The conversion of low entropy $Q_{s,net}$ to high entropy heat at the surface, σ_{QS}, equals:

$$\sigma_{QS} = Q_{S,net}\left(\frac{1}{T_{surf}} - \frac{1}{T_{sun}}\right) \quad (2)$$

where T_{sun} is the sun surface temperature, approximated here to be 5780 K, and T_{surf} is the radiometric surface temperature, calculated from $Q_{L,out}$ using the Stefan-Boltzmann equation:

$$T_{surf} = \left(\frac{Q_{L,out}}{A\varepsilon_{surf}C}\right)^{1/4} \quad (3)$$

in which *C* is the Stefan-Boltzmann constant and the view factor *A* is assumed to be one. The surface emissivity, ε_{surf}, was calculated following Juang *et al.* [22] and Chen and Sun-Mack [23]:

$$\varepsilon_{surf} = 0.99 - 0.16\alpha \quad (4)$$

where is the shortwave albedo, calculated here as the monthly average of noontime $Q_{S,out}$ divided by $Q_{S,in}$.

Ecosystem entropy production from $Q_{L,in}$ and subsequent production of heat, σ_{QL}, can likewise be calculated:

$$\sigma_{QL} = Q_{L,net}\left(\frac{1}{T_{surf}} - \frac{1}{T_{sky}}\right) \quad (5)$$

The sky temperature, T_{sky}, was calculated from $Q_{L,in}$ using the Stefan-Boltzmann equation:

$$T_{sky} = \left(\frac{Q_{L,in}}{A\varepsilon_{sky}C}\right)^{1/4} \quad (6)$$

The emissivity of the sky, ε_{sky}, was assumed to be 0.85 [24] and *A* is again assumed to be one. σ is then the sum of σ_{QS} and σ_{QL}:

$$\sigma = \sigma_{QS} + \sigma_{QL} \quad (7)$$

All entropy production terms are calculated on the native half hourly or hourly time scales of the radiometric and micrometeorological measurements from the FLUXNET database as described below.

It is important to note that we are studying entropy production owing to radiative terms here, rather than total ecosystem entropy production, which includes hydrologic and metabolic terms [15] that are not measured, cannot easily be measured, or may be erroneously measured using standard micrometeorological and eddy covariance observations. A study of overall ecosystem-atmosphere

entropy budget is excluded for three reasons. One is that the entropy production owing to H requires an estimate of the aerodynamic surface temperature, which is different from T_{surf} and is difficult to measure. Entropy production owing to LE is discussed by Kleidon [25], and requires an estimate of boundary layer relative humidity, which is not measured by standard eddy covariance instrumentation (although relative humidity in or above the canopy typically is). Another complication arises because the surface-atmosphere energy balance is rarely closed by the eddy covariance method, likely due to an underestimation of sensible and/or latent heat flux [26,27] or partial measurements of G [28]. Energy balance closure tends to differ among different ecosystem types [26], and cross-biome studies of hydrologic entropy production may be biased for this reason. In addition, metabolic terms can only be approximated from eddy covariance measurements of the net ecosystem exchange of CO_2; estimates of photosynthesis and respiration remain difficult to model using eddy covariance observations. In brief, we are studying the ability of ecosystems to absorb low-entropy solar energy and convert this energy to high-entropy radiative heat. We refer the reader to Brunsell *et al.* [21] for a further discussion of ecosystem-atmosphere entropy flux.

2.3. Empirical Maximum Entropy Production (EMEP)

To address the experimental hypotheses, we wish to quantify the difference between observed radiative ecosystem entropy production and the maximum radiative entropy production that an ecosystem can produce. We provide an empirical estimate of maximum entropy production, EMEP, by considering the maximum amount of entropy that the terrestrial surface could produce under ideal conditions.

Ecosystems never absorb all incident shortwave energy, but some coniferous ecosystems have α values less than 0.05 [29]. α cannot be less than zero, and $Q_{S,net}$ approaches $Q_{S,in}$ as approaches zero. Therefore, when estimating the maximum radiative entropy that an ecosystem can produce, we assume that the $Q_{S,net}$ term of Equation (2) equals $Q_{S,in}$.

The temperature of the surface under a radiation load will exceed that of the atmosphere under normal circumstances, unless all the incident energy is used to evaporate water and produce LE, is partitioned into G and M, or there is a net lateral input of heat into the atmosphere. In other words, T_{surf} approaches T_{air} if the temperature of the surface is not increasing to produce H, regardless of the distinction between aerodynamic and radiometric surface temperatures. We assume that replacing T_{surf} with T_{air} in Equation (2), in addition to replacing $Q_{S,net}$ with $Q_{S,in}$, results in the maximum value of σ_{Qs} ($\sigma_{Qs,\max}$):

$$\sigma_{QS,\max} = Q_{S,in}\left(\frac{1}{T_{air}} - \frac{1}{T_{sun}}\right) \tag{8}$$

T_{sky} is typically smaller than T_{air}, and we find it unrealistic for ecosystem surface temperature to reach T_{sky} when surrounded by air as T_{surf} is usually greater than T_{air}. Under these conditions, the maximum entropy due to longwave radiation flux, $\sigma_{QL,\max}$ is:

$$\sigma_{QL,\max} = Q_{L,net}\left(\frac{1}{T_{surf}} - \frac{1}{T_{air}}\right) \tag{9}$$

which is a small number compared to $\sigma_{QS,\max}$—often less than two orders of magnitude less than $\sigma_{QS,\max}$—and often negative [21]. Furthermore, the assumption that $T_{surf} = T_{air}$ drives Equation (9) to zero. We therefore assume that the empirical maximum entropy production, EMEP, equals $\sigma_{QS,\max}$ and again emphasize that we are investigating radiative contributions to total ecosystem entropy production in this analysis.

2.4. Ecosystem Observations: Duke Forest

We test the experimental hypothesis that ecosystem radiative entropy production increases during the initial stages of ecosystem succession then decreases as ecosystems age [7] using micrometeorological measurements from the Duke Forest, NC, USA [22,30,31] (Table 1). The experimental ecosystems model a successional trajectory following agricultural abandonment in the southeastern United States [32]: an old field (OF) ecosystem dominated by grasses and forbs [33] is replaced on decadal time scales by early successional trees, here a *Pinus taeda* forest (hereafter abbreviated PP), which are then replaced by hardwood vegetation (HW, [34]) on time scales of approximately a century. All Duke Forest ecosystems were equipped with eddy covariance and micrometeorological measurements. T_{air} was measured at 2 m height at OF and at 2/3 canopy height at PP and HW. Radiometric measurements were made at 2.0 m in OF, at 21.2 m in PP, and at 41.8 m in HW [30]. Incident and outgoing shortwave and longwave measurements are available for 2004, a year with normal precipitation, and 2005, a drought year [22,30,35].

Table 1. Location, Köppen-Geiger climate classification, IGBP vegetation type, years of available measurement, and ecosystem entropy production (σ) as a fraction of empirical maximum entropy production (EMEP) of the 64 sites in the Free/Fair-Use FLUXNET database with partitioned incident and outgoing radiation flux measurements.

Site	σ/EMEP	Veg.[a]	Clim.[b]	Year(s)	Lat.	Long.	Ref.
AUFog	0.71	WET	TR	2006–2007	−12.5425	131.3070	[36]
AUHow	0.70	SAV	TR	2001–2006	−12.4943	131.1520	[37]
AUWac	0.83	EBF	T	2005–2007	−37.4290	145.1870	[38]
BRSa3	0.91	EBF	TR	2000–2003	−3.01803	−54.9714	[39]
BWGhg	0.69	SAV	D	2003	−21.51	21.74	[40]
BWGhm	0.68	SAV	D	2003	−21.20	21.75	[40]
BWMa1	0.79	SAV	D	1999–2001	−19.9155	23.5605	[41]
CAMer	0.67	WET	TC	2003–2004	45.4094	−75.5186	[42]
CAQcu	0.70	ENF	B	2004–2006	49.2671	−74.0365	[43]
CAQfo	0.84	ENF	B	2003–2005	49.6925	−74.3421	[44]
CASF1	0.77	ENF	B	2003–2005	54.4850	−105.8180	[45]
CASF2	0.68	ENF	B	2003–2005	54.2539	−105.8780	[46,47]
CASF3	0.57	OSH	B	2003–2005	54.0916	−106.0050	[46,47]
CHOe1	0.68	GRA	T	2003–2006	47.2856	7.7321	[48]
CHOe2	0.58	CRO	T	2005	47.2860	7.7340	[49]
CZwet	0.83	WET	T	2006	49.0250	14.7720	[50]
EGeb	0.74	CRO	T	2004–2006	51.1001	10.9143	[51]

Table 1. *Cont.*

Site	σ/EMEP	Veg.[a]	Clim.[b]	Year(s)	Lat.	Long.	Ref.
DEGri	0.84	GRA	T	2006	50.9495	13.5125	[52]
DEHai	0.79	DBF	T	2004–2006	51.0793	10.4520	[53]
DEKli	0.66	CRO	T	2004–2006	50.8929	13.5225	[52]
DEMeh	0.72	GRA	T	2003–2006	51.275	10.6555	[54]
DETha	0.93	ENF	T	2004–2006	50.9636	13.5669	[55]
DEWet	0.89	ENF	T	2002–2006	50.4535	11.4575	[56]
ESES2	0.78	CRO	S	2005–2006	39.2755	−0.3152	[57]
ESLMa	0.72	ENF	B	2005–2006	39.9415	−5.7734	[58]
ESVDA	0.68	WET	B	2005–2006	42.1522	1.4485	[59]
FRFon	0.77	DBF	T	2005–2006	48.4763	2.7801	[60]
FRLBr	0.80	ENF	T	2003–2006	44.7171	−0.7693	[61]
FRPue	0.76	EBF	S	2005–2006	43.7414	3.5958	[62]
IEDri	0.70	GRA	T	2003–2005	51.9867	−8.7518	[63]
ILYat	0.76	ENF	D	2004–2005	31.3450	35.0515	[64]
ITAmp	0.65	GRA	S	2005–2006	41.9041	13.6052	[65]
ITBCi	0.71	CRO	S	2006	40.5238	14.9574	[66]
ITCas	0.69	CRO	S	2006	45.0628	8.6685	[67]
ITLav	0.85	ENF	T	2004, 2006	45.9553	11.2812	[68]
ITMBo	0.56	GRA	T	2004–2006	46.0156	11.0467	[69]
ITRen	0.85	ENF	T	2004–2006	46.5878	11.4347	[70]
ITRo1	0.67	DBF	S	2005–2006	42.4081	11.9300	[71]
ITSRo	0.88	ENF	S	2004, 2006	43.7279	10.2844	[72]
NLCa1	0.67	GRA	T	2003–2006	51.9710	4.9270	[73]
NLLan	0.73	CRO	T	2005–2006	51.9536	4.9029	[74]
NLLoo	0.82	ENF	T	1999–2000, 2002–2006	52.1679	5.7440	[75]
NLLut	0.72	CRO	T	2006	53.3989	6.3560	[74]
NLMol	0.86	CRO	T	2005	51.650	4.6390	[74]
PLwet	0.77	WET	T	2004–2005	52.7622	16.3094	[76]
PTMi2	0.59	GRA	S	2004–2006	38.4765	−8.0246	[77]
RUCok	0.73	OSH	B	2003–2005	70.6167	147.8830	[78]
RUFyo	0.91	ENF	TC	1998–2004	56.4617	32.9240	[79]
RUZot	0.79	ENF	B	2002–2004	60.8008	89.3508	[80]
SENor	0.95	ENF	TC	2005	60.0865	17.4795	[81]
SESk2	0.84	ENF	T	2004–2005	60.1297	17.8401	[82]
UKPL3	0.72	DBF	T	2005–2006	51.4500	−1.2667	[83]
USARM	0.31	CRO	S	2003–2006	36.6058	−97.4888	[84]
USAud	0.60	GRA	D	2002–2006	31.5907	−110.51	[85]
USBkg	0.86	GRA	TC	2004–2006	44.3453	−96.8362	[86]
USBo1	0.78	CRO	TC	2001–2007	40.0062	−88.2924	[87]
USDk1	0.78	GRA	S	2004–2005	35.9712	−79.0934	[33]
USDk2	0.85	DBF	S	2004–2005	35.9736	−79.1004	[34]
USDk3	0.88	ENF	S	2004–2005	35.9782	−79.0942	[88]

Table 1. *Cont.*

Site	σ/EMEP	Veg.[a]	Clim.[b]	Year(s)	Lat.	Long.	Ref.
USFPe	0.63	GRA	D	2001–2006	48.3077	−105.1019	[89]
USGoo	0.84	GRA	S	2002–2006	34.2547	−89.8735	[90]
USMMS	0.77	DBF	T	2002–2004	39.3231	−86.4131	[91]
USMOz	0.93	DBF	T	2004–2006	38.7441	−92.2000	[92]
USWCr	0.72	DBF	TC	1999–2006	45.8059	−90.0799	[93]

[a] Veg. = vegetation following the International Geosphere-Biosphere Programme (IGBP) classification. DBF: deciduous broadleaf forest, ENF: evergreen needleleaf forest, GRA: grassland, MF: mixed forest, OSH: open shrubland, WET: wetland; [b] Climate group following the Köppen–Geiger classification scheme. A: Arctic, B: Boreal, D: Dry, S: Subtropical-Mediterranean, T: Temperate, TC: Temperate-Continental, TR: Tropical.

2.5. Ecosystem Observations: FLUXNET

To quantify biogeographic patterns of ecosystem entropy production in relation to EMEP, we analyzed micrometeorological and eddy covariance data from 64 tower sites in the FLUXNET Free/Fair Use database [94] (Figure 2, Tables 1 and 2), including the Duke Forest ecosystems, for which R_n, $Q_{L,in}$, and $Q_{L,out}$ measurements were available. Site names, geographic coordinates, climate type, and ecosystem type after the International Geosphere-Biosphere Programme (IGBP) classification are listed in Table 1 and summarized in Table 2. Woody savannas and savannas were combined to form a single class called "savanna". The study sites did not include any Arctic ecosystems or ecosystems classified as mixed forests: both PP and HW consist of mixed coniferous and deciduous vegetation, but PP is dominated by conifers and HW by deciduous species.

Figure 2. A global map of the 64 Free/Fair-Use eddy covariance research sites in the FLUXNET database with available incident and outgoing longwave radiation flux measurements, including detailed maps of portions of North America and Europe with high tower density. Abbreviations follow Table 1.

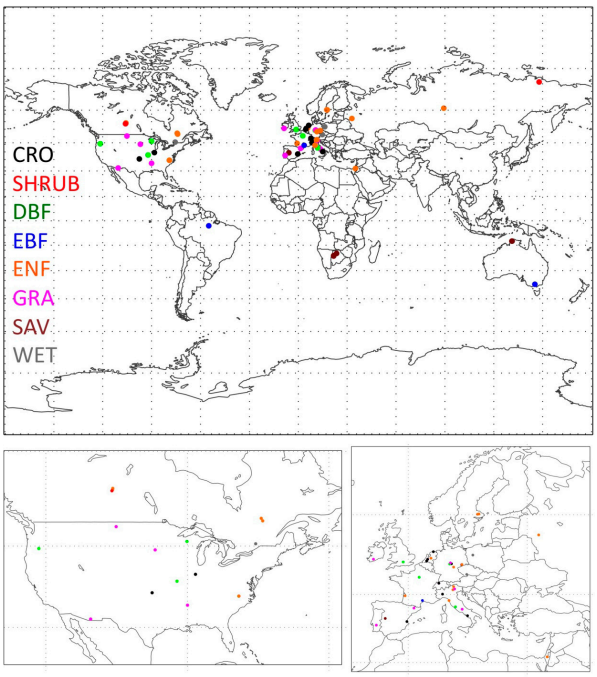

Table 2. Summary table of the number of site-years of eddy covariance data available per vegetation and climate class in the Free Fair-Use FLUXNET database for sites with available outgoing longwave radiation measurements. Abbreviations follow Table 1.

	T	TC	TR	D	B	A	S	Sum
CRO	6	1	0	0	0	0	4	11
OSH	0	0	0	0	2	0	0	2
DBF	3	1	0	0	0	0	4	8
EBF	1	0	1	0	0	0	1	3
ENF	7	2	0	1	5	0	2	17
GRA	7	1	0	2	0	0	4	14
MF	0	0	0	0	0	0	0	0
SAV	0	0	1	3	0	0	1	5
WET	2	1	1	0	0	0	0	4
Sum	26	6	3	6	7	0	16	64

2.6. Data Quality and Gapfilling

$Q_{S,in}$ and $Q_{S,out}$ were not available in the FLUXNET database, excluding the Duke Forest ecosystems. $Q_{S,in}$ was assumed to follow an empirical relationship with the photosynthetically active photon flux density, PPFD, $Q_{S,in} = c\text{PPFD}$, where c is an empirical coefficient determined to be 0.5357 J μmol^{-1} using observations of $Q_{S,in}$ and PPFD from the Duke Forest. We note that the precise value of c varies as a function of atmospheric transmissivity to shortwave radiation, which includes PPFD, and this uncertainty will introduce minor errors in the FLUXNET analysis. Following the measurement or estimation of $Q_{S,in}$, $Q_{S,out}$ was calculated by difference using Equation (1). Only measured quantities of R_n, $Q_{L,in}$, $Q_{L,out}$, and PPFD were used in the analysis of the FLUXNET ecosystems: no gapfilling was performed and no gapfilled data products were used. In the case of the Duke Forest sites, the close correlation between meteorological variables measured at the three sites permits accurate gapfilling [33], and we gapfilled missing micrometeorological measurements using linear relationships with adjacent sensors [30] to obtain continuous two year time series of σ and EMEP and to calculate annual sums of these quantities.

2.7. Statistical Analyses

We anticipate that the temperature and radiation flux variables associated with σ and EMEP follow known geographic patterns and that a statistical analysis of σ and EMEP in response to temperature and radiation would principally reveal geographic effects. The experimental hypotheses concern the degree to which observed σ approaches an empirical maximum along succession and with respect to vegetation and climate characteristics. Therefore, we focus our analysis on the fraction of EMEP realized by σ, σ/EMEP (Figure 3), and performed individual one-way analyses of variance (ANOVA) to quantify if σ/EMEP is significantly different by climate or vegetation type (Table 2) using R (R Development Core Team). Tukey's Honestly Significant Difference (HSD) *post-hoc* test was performed if main effects were adjudged to be significant at the 95% confidence level.

Figure 3. A typical diurnal course of empirical maximum entropy production (EMEP) in a terrestrial ecosystem. In this analysis, we ask if measured ecosystem entropy production (σ, here for the old field (OF), planted pine (PP) and hardwood forest (HW) ecosystems in the Duke Forest) approach EMEP, and what are the ecosystem-level attributes that contribute to a high σ/EMEP?

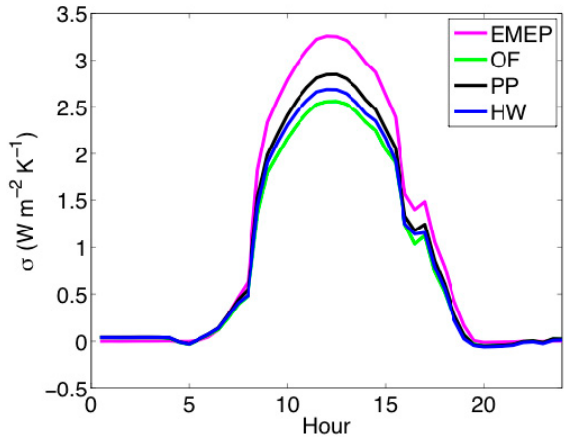

3. Results

3.1. Entropy Production along Ecological Succession: Duke Forest

σ/EMEP averaged 0.75 at OF, 0.87 at PP, and 0.83 at HW (Table 1, Figures 4 and 5) and differed by less than 1% between years among the different vegetation types. EMEP was assumed to be equal among the adjacent Duke Forest ecosystems, and was 3% higher during the drought year of 2005 due to higher $Q_{S,in}$. Mean T_{air} differed by less than 0.02 °C between the two years, within the range of uncertainty of the temperature sensors in a field setting.

$Q_{S,net}$ at OF during the two year measurement period was 8790 MJ·m^{-2}, 89% of that at PP (9824 MJ·m^{-2}) and 93% of that at HW (9471 MJ·m^{-2}), due to the higher albedo at OF [22,95]. Mean T_{surf} was 17.1 °C at OF, 15.8 °C at PP, and 16.3 °C at HW (Figure 6). As a result, $(1/T_{surf} - 1/T_{sun})$ differed among ecosystems, but by less than 1%. In other words, differences in σ and therefore σ/EMEP among ecosystems were dominated by differences in $Q_{s,net}$ rather than difference in T_{surf}.

When considering seasonal patterns, σ/EMEP was consistently lower in OF, particularly during the winter months (Figure 5). These differences were due in part to $Q_{S,net}$ values at OF that were lower than its forest counterparts by *ca*. 1 MJ m^{-2} day^{-1} (Figure 6) during winter.

The quantity $(1/T_{surf} - 1/T_{sun})$ tended to be lower during the summer months at OF *versus* PP and HW, but again only by a fraction of a percent (Figure 7). σ/EMEP at HW decreased slightly during the leaf out period in spring when high-albedo young leaves emerged [22] (Figure 5). σ/EMEP at PP varied by only a few percent seasonally and was consistently higher than σ/EMEP at the other Duke Forest ecosystems (Figure 5).

Figure 4. The cumulative sums of empirical maximum entropy production (EMEP) and observed entropy production (σ) at the Duke Forest old field (OF), planted pine (PP) and hardwood forest (HW) ecosystems during 2004 (left) and 2005.

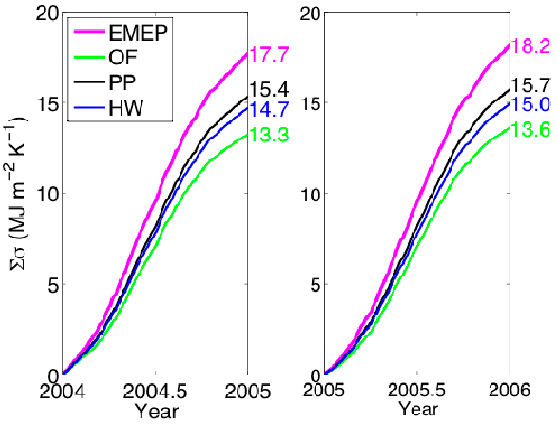

Figure 5. The daily sum of entropy production (σ) divided by the daily sum of empirical maximum entropy production (EMEP) at the Duke Forest old field (OF), planted pine (PP) and hardwood forest (HW) sites, smoothed using a twenty day digital filter.

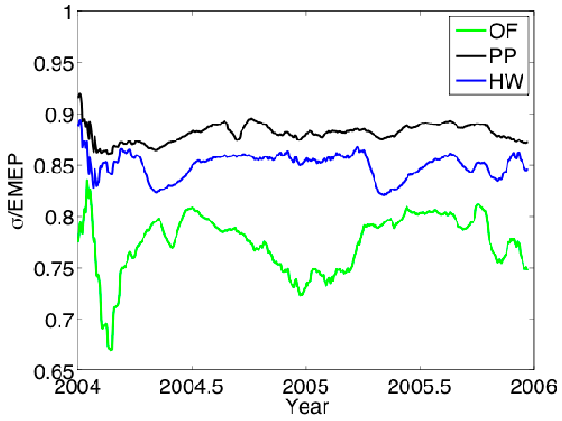

Figure 6. Daily average net shortwave radiation ($Q_{S,net}$) for the Duke Forest old field (OF), planted pine (PP) and hardwood forest (HW) ecosystems smoothed using a ten-day digital filter.

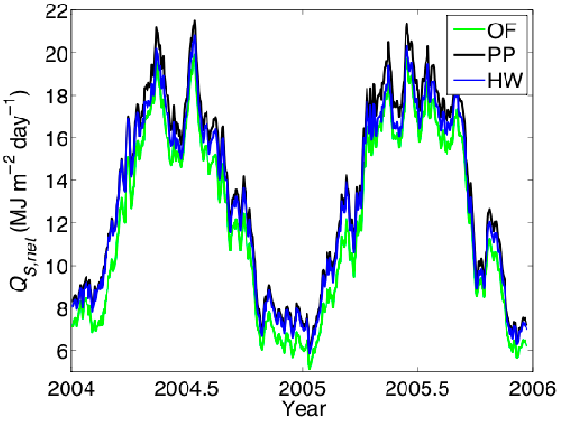

Figure 7. Daily averages of the temperature term of ecosystem entropy production for shortwave radiation, $1/T_{surf} - 1/T_{sun}$ (see Equation (2)), at the Duke Forest old field (OF), planted pine (PP) and hardwood forest (HW) sites, smoothed using a twenty day digital filter.

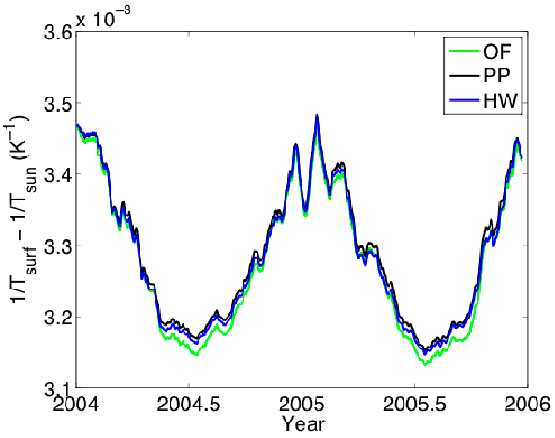

Figure 8. Box and whisker plots of entropy production (σ) per empirical maximum entropy production (EMEP) for the Free/Fair Use FLUXNET sites described in Tables 1 and 2. Subplot A displays results per climate type and subplot B per vegetation type. Subplot C is the same as subplot B, but combining all forests into a single classification called "FOR". Abbreviations follow Table 1. The distribution of σ/EMEP did not differ significantly among climate types (subplot A), but significant differences were observed among vegetation types.

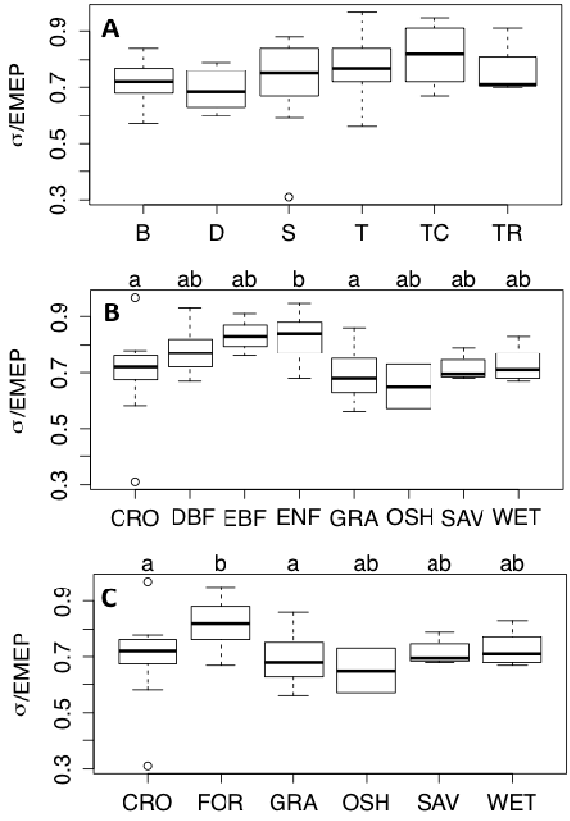

3.2. Entropy Production as a Function of Climate and Vegetation Type: FLUXNET

σ/EMEP across the FLUXNET ecosystems averaged 0.75 with a standard deviation of 0.11, and did not differ among different climate classifications (Figure 8A). σ/EMEP was higher in evergreen needleleaf forests (mean σ/EMEP = 0.83) than in croplands (mean σ/EMEP = 0.70) and grasslands (mean σ/EMEP = 0.70) at the 95% confidence level (Figure 8B). The mean σ/EMEP of croplands and grasslands was lower than forests when all forest classes were combined (mean σ/EMEP = 0.81, Figure 8C). σ itself rarely exceeded *ca*. 2 W m^{-2} K^{-1} (Figure 9), even during peak daytime hours.

Figure 9. Kernel density estimates of ecosystem radiative entropy production, for all of the daytime observations of the Free/Fair Use database (defined as periods when the local zenith angle was less than 90°, Table 1), and for noontime observations only.

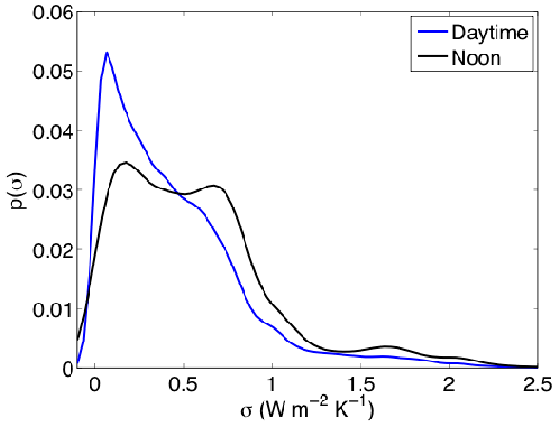

4. Discussion

σ increased then decreased along ecological succession in the Duke Forest ecosystems (Figure 4), and was negatively correlated with albedo. However, the largest value of σ, observed in the early successional planted pine forest, was only 89% of EMEP, suggesting that even this fast-growing pine forest is unable to effectively capture and dissipate all available energy due to a non-zero albedo. These results are consistent with the meta-analysis of the FLUXNET sites, which revealed that σ/EMEP was lowest in grassland and cropland ecosystems and higher in forested ecosystems. Interestingly, the ecosystems associated with σ/EMEP values greater than 0.90 were an old growth forest in Germany (DE-Tha [55]), a mature tropical forest in Brazil (BR-Sa3 [39]), evergreen needleleaf forests in Russia (RUFyo [79]) and Sweden (SE-Sk2 [82]), and a mature deciduous forest in the Ozarks (US-MOz [92]) (Table 1). In other words, ecosystems commonly characterized as late-successional or "climax", as well as evergreen needleleaf forests, tended to exhibit the highest values of σ /EMEP. Further, observations demonstrate that σ values greater than *ca* 0.2 W m^{-2} K^{-1} are rare (Figure 9), noting that our analysis excluded entropy production owing to hydrologic or metabolic terms.

It is important to mention that the EMEP assumes that there is no lateral exchange of energy (Figure 1) and as such is not a complete description of energy flows into and out of the spatial domain measured by the radiometers and eddy covariance instrumentation, noting that net lateral heat fluxes are likely to be small [96]. Additionally, the EMEP as defined here only reflects radiative entropy production by the surface, and does not consider the impact of these surface energy and entropy fluxes within the

Earth system [97,98]. By providing insight into entropy production of different vegetation types, we hope to contribute to a greater understanding of the total global entropy production to better couple environmental and Earth systems sciences.

These results support elements the seminal work of Lotka [3] on energy capture. Our results demonstrate the central importance of albedo in determining ecosystem energy gain and in closing the imbalance between σ and EMEP. Maintaining a cool T_{surf} near T_{air} is important for increasing entropy production (Equation (1)), but the impact of pathways with which to dissipate energy is minor in the entire σ budget compared to the impacts of $Q_{S,net}$, which differed on the order of a MJ day^{-1} in the case of the adjacent Duke ecosystems (Figure 6). Although forested ecosystems often have a cool T_{surf} compared to their non-forested counterparts, due largely to enhanced sensible and latent heat fluxes despite lower albedo [22,99], the dominant term in the σ budget is due to energy gain rather than efficient energy dissipation via the terms that contribute to T_{surf} (see Equation (1)). As terrestrial ecosystems capture more energy with ecosystem development, they have the opportunity to dissipate more of it and increase σ.

σ itself approaches, but does not reach, a "maximum" state, which to be fair cannot be reached by terrestrial ecosystems with non-zero albedo. As ecosystem albedo values are rarely less than 0.05 [29], at least 5% of potential σ is lost. As the mature forests are able to capture more shortwave radiation, the role of succession in controlling σ cannot be ignored. At the same time, results do not point to a simple or generalizable decrease in σ at older stages of ecosystem development. Coupled to findings that older ecosystems can sequester considerable CO_2 [100], our results suggest that formally incorporating ecosystem retrogression into theories of ecosystem development may overgeneralize the behavior of successional trajectories.

It is also important to note that ecosystems with σ values greater than 90% of EMEP existed in areas that are not prone to pronounced water limitation. In other words, water limited ecosystems that are unable to develop a dense canopy with low albedo will produce less entropy, which introduces an important biogeographic component to global ecosystem σ production. As climate continues to change and atmospheric [CO_2] continues to increase, regional hydrology may change in a way that increases or decreases radiative σ.

Links between climate change, hydrology, and ecosystem thermodynamics have yet to be explored, nor has the role of human management and its tendency to shift ecosystems to an earlier successional stage [101] or a later successional stage with active disturbance management like fire suppression. Ecosystem entropy production has practical consequences for maintaining a cool surface as a buffer against the impacts of climate change [102,103], but research to date tends to focus on theory. Empirical and modeling studies on ecosystem entropy production can complement theoretical developments for a comprehensive view of the role of ecosystem dynamics in the earth system in an era of global changes to the planetary energy budget. For a more complete view of total ecosystem entropy production, future studies may consider including hydrologic and metabolic contributions, and extend beyond the plot scale to further investigate the role that the entropy production of different ecosystems plays in an Earth system context.

5. Conclusions

Using data from successional chronosequence in the Duke Forest and other established Fluxnet sites, we tested the hypothesis that entropy production should increase then decrease along a successional trajectory. From this exercise we have found that:

- Ecosystem energy gain via (lower) shortwave albedo is the most relevant component for forcing ecosystem entropy production closer to its empirical maximum value;
- Entropy production was higher at a pine plantation in the Duke Forest, representative of an intermediate successional stage, than a grass field, representing early succession, and hardwood vegetation, meant to approximate a later successional stage. These results lend support to the notion that ecosystem entropy production may increase then decrease along succession [7], but FLUXNET observations suggest that older-successional ecosystems often have the highest entropy production with respect to an estimated maximum, lending support to the model of Skene [5].
- Further results from the FLUXNET analysis suggest that the relationship between succession and entropy production depends on vegetation characteristics, and late successional ecosystems frequently exhibited high values of σ/EMEP.
- Empirical and modeling studies of ecosystem entropy production may provide relevant insights on how ecosystems might maintain a cool surface as a buffer against the impacts of climate change, and how human management may improve or impede the important ecosystem service of microclimate regulation.

Acknowledgments

This work used eddy covariance data acquired by the FLUXNET community and in particular by the following networks: AmeriFlux (U.S. Department of Energy, Biological and Environmental Research, Terrestrial Carbon Program (DE-FG02-04ER63917 and DE-FG02-04ER63911)), AfriFlux, AsiaFlux, CarboAfrica, CarboEuropeIP, CarboItaly, CarboMont, ChinaFlux, Fluxnet-Canada (supported by CFCAS, NSERC, BIOCAP, Environment Canada, and NRCan), GreenGrass, KoFlux, LBA, NECC, OzFlux, TCOS-Siberia, USCCC. We acknowledge the financial support to the eddy covariance data harmonization provided by CarboEuropeIP, FAO-GTOS-TCO, iLEAPS, Max Planck Institute for Biogeochemistry, National Science Foundation, University of Tuscia, Université Laval and Environment Canada, and US Department of Energy and the database development and technical support from Berkeley Water Center, Lawrence Berkeley National Laboratory, Microsoft Research eScience, Oak Ridge National Laboratory, University of California—Berkeley, University of Virginia. Michael Kleder of Delta Epsilon Technologies, LLC for provided the MATLAB code for the world map with political boundaries. PCS additionally acknowledges funding from the National Science Foundation (*"Scaling Ecosystem Function: Novel Approaches from MaxEnt and Multiresolution"*, Division of Biological Infrastructure #1021095). LH acknowledges the Applied Fundamental Research Program of Yunnan Province (2013FB078) and the Chinese Academy of Sciences scholarship for international cooperation. The authors thank Subodh Adhikari, Michael Bestwick, Badamgarav Dovchin, Elizabeth S.K. Harris, Aiden Johnson, Nar Ranabhat, Deicy Sanchez Espinoza, and Angela Tang for constructive comments on the manuscript, and Amy Trowbridge for statistical advice.

Author Contributions

Paul C. Stoy conceived of the study, analyzed the data, and wrote the manuscript with all coauthors. Paul C. Stoy, Kimberly A. Novick, Jehn-Yih Juang and Mario B. S. Siqueira contributed data from the Duke Forest ecosystems. All authors have read and approved the final manuscript.

Conflicts of Interest

The authors declare no conflict of interest.

References

1. Schrödinger, E. *What Is Life? With Mind and Matter and Autobiographical Sketches*; Cambridge University Press: Cambridge, UK, 1992.
2. Schneider, E.D.; Kay, J.J. Life as a manifestation of the second law of thermodynamics. *Math. Comput. Model.* **1994**, *19*, 25–48.
3. Lotka, A.J. Contribution to the energetics of evolution. *Proc. Natl. Acad. Sci. USA* **1922**, *8*, 147–151.
4. Prigogine, I. *Introduction to Thermodynamics of Irreversible Processes*, 2nd ed.; Interscience Publishers: New York, NY, USA, 1961; p. 119.
5. Skene, K.R. The energetics of ecological succession: A logistic model of entropic output. *Ecol. Model.* **2013**, *250*, 287–293.
6. Kleidon, A.; Malhi, Y.; Cox, P.M. Maximum entropy production in environmental and ecological systems. *Philos. Trans. R. Soc. B Biol. Sci.* **2010**, *365*, 1297–1302.
7. Holdaway, R.J.; Sparrow, A.D.; Coomes, D.A. Trends in entropy production during ecosystem development in the Amazon Basin. *Philos. Trans. R. Soc. B Biol. Sci.* **2010**, *365*, 1437–1447.
8. Celeste, L.; Pignatti, S. Analysis of the chorological diversity in some South-European vegetational series. *Annali di Bot* **1988**, *46*, 25–34.
9. Lin, H.; Cao, M.; Zhang, Y. Self-organization of tropical seasonal rain forest in southwest China. *Ecol. Model.* **2011**, *222*, 2812–2816.
10. Ludovisi, A. Biotic and abiotic entropy production in lake ecosystems. *Ecol. Model.* **2004**, *179*, 145–147.
11. Ludovisi, A.; Poletti, A. Use of thermodynamic indices as ecological indicators of the development state of lake ecosystems. 1. Entropy production indices. *Ecol. Model.* **2003**, *159*, 203–222.
12. Meysman, F.J.R.; Bruers, S. A thermodynamic perspective on food webs: Quantifying entropy production within detrital-based ecosystems. *J. Theor. Biol.* **2007**, *249*, 124–139.
13. Aoki, I. Entropy production in living systems: From organisms to ecosystems. *Thermochim. Acta* **1995**, *250*, 359–370.
14. Aoki, I. Hololological study of lakes from an entropy viewpoint—Lake Mendota. *Ecol. Model.* **1989**, *45*, 81–93.
15. Unrean, P.; Srienc, F. Metabolic networks evolve towards states of maximum entropy production. *Metab. Eng.* **2011**, *13*, 666–673.
16. Jaynes, E.T. Information theory and statistical mechanics. *Phys. Rev.* **1957**, *106*, 620–630.

17. Ulanowicz, R.E. An hypothesis on the development of natural communities. *J. Theor. Biol.* **1980**, *85*, 223–245.
18. Ulanowicz, R.E.; Hannon, B.M. Life and the production of entropy. *Proc. R. Soc. London Ser. B* **1987**, *232*, 181–192.
19. Jørgensen, S.E.; Marques, J.C.; Müller, F.; Nielsen, S.N.; Patten, P.C.; Tiezzi, E.; Ulanowicz, R.E. *A New Ecology: Systems Perspective*; Elsevier: New York, NY, USA, 2007; p. 275.
20. Odum, E.P. The strategy of ecosystem development. *Science* **1969**, *164*, 262–270.
21. Brunsell, N.A.; Schymanski, S.J.; Kleidon, A. Quantifying the thermodynamic entropy budget of the land surface: Is this useful? *Earth Syst. Dyn.* **2011**, *2*, 87–103.
22. Juang, J.-Y.; Katul, G.G.; Siqueira, M.B.S.; Stoy, P.C.; Novick, K.A. Separating the effects of albedo from eco-physiological changes on surface temperature along a successional chronosequence in the southeastern US. *Geophys. Res. Lett.* **2007**, *34*, L21408.
23. Chen, Y.; Sun-Mack, S. Surface Spectral Emissivity Derived from MODIS Data. In Proceedings of the SPIE 3rd International Asia-Pacific Environmental Remote Sensing Symposium 2002: Remote Sensing of the Atmosphere, Ocean, Environment, and Space, Hangzhou, China, 23–27 October 2002.
24. Campbell, G.S.; Norman, J.M. *An Introduction to Environmental Biophysics*, 2nd ed.; Springer: New York, NY, USA, 1998.
25. KleIdon, A. A model of surface heat fluxes based on the theory of maximum entropy production. *Soil. Water Res.* **2008**, *3*, S89–S94.
26. Stoy, P.C.; Mauder, M.; Foken, T.; Marcolla, B.; Boegh, E.; Ibrom, A.; Arain, M.A.; Arneth, A.; Aurela, M.; Bernhofer, C.; *et al.* A data-driven analysis of energy balance closure across FLUXNET research sites: The role of landscape scale heterogeneity. *Agric. For. Meteorol.* **2013**, *171*, 137–152.
27. Foken, T. The energy balance closure problem: An overview. *Ecol. Appl.* **2008**, *18*, 1351–1367.
28. Leuning, R.; van Gorsel, E.; Massman, W.J.; Isaac, P.R. Reflections on the surface energy imbalance problem. *Agric. For. Meteorol.* **2012**, *156*, 65–74.
29. Hollinger, D.Y.; Ollinger, S.V.; Richardson, A.D.; Meyers, T.; Dail, D.B.; Martin, M.E.; Scott, N.A.; Arkebauer, T.J.; Baldocchi, D.D.; Clark, K.L.; *et al.* Albedo estimates for land surface models and support for a new paradigm based on foliage nitrogen concentration. *Glob. Chang. Biol.* **2009**, *16*, 696–710.
30. Stoy, P.C.; Katul, G.G.; Siqueira, M.B.S.; Juang, J.-Y.; McCarthy, H.R.; Oishi, A.C.; Uebelherr, J.M.; Kim, H.-S.; Oren, R. Separating the effects of climate and vegetation on evapotranspiration along a successional chronosequence in the southeastern U.S. *Glob. Chang. Biol.* **2006**, *12*, 2115–2135.
31. Stoy, P.C.; Katul, G.G.; Siqueira, M.B.S.; Juang, J.-Y.; Novick, K.; McCarthy, H.R.; Oishi, A.C.; Oren, R. Role of vegetation in determining carbon sequestration along ecological succession in the southeastern United States. *Glob. Chang. Biol.* **2008**, *14*, 1409–1427.
32. Oosting, H.J. An ecological analysis of the plant communities of Piedmont, North Carolina. *Am. Midl. Nat.* **1942**, *28*, 1–126.
33. Novick, K.A.; Stoy, P.C.; Katul, G.G.; Ellsworth, D.S.; Siqueira, M.B.S.; Juang, J.; Oren, R. Carbon dioxide and water vapor exchange in a warm temperate grassland. *Oecologia* **2004**, *138*, 259–274.

34. Pataki, D.E.; Oren, R. Species differences in stomatal control of water loss at the canopy scale in a mature bottomland deciduous forest. *Adv. Water Resour.* **2003**, *26*, 1267–1278.
35. Stoy, P.C.; Katul, G.G.; Siqueira, M.B.S.; Juang, J.-Y.; Novick, K.A.; Uebelherr, J.M.; Oren, R. An evaluation of models for partitioning eddy covariance-measured net ecosystem exchange into photosynthesis and respiration. *Agric. For. Meteorol.* **2006**, *141*, 2–18.
36. Guerschman, J.P.; van Dijk, A.I.J.M.; Mattersdorf, G.; Beringer, J.; Hutley, L.B.; Leuning, R.; Pipunic, R.C.; Sherman, B.S. Scaling of potential evapotranspiration with MODIS data reproduces flux observations and catchment water balance observations across Australia. *J. Hydrol.* **2009**, *369*, 107–119.
37. Hutley, L.B.; O'Grady, A.P.; Eamus, D. Evapotranspiration from Eucalypt open-forest savanna of Northern Australia. *Funct. Ecol.* **2000**, *14*, 183–194.
38. Martin, D.; Beringer, J.; Hutley, L.B.; McHugh, I. Carbon cycling in a mountain ash forest: Analysis of below ground respiration. *Agric. For. Meteorol.* **2007**, *147*, 58–70.
39. Saleska, S.R.; Miller, S.D.; Matross, D.M.; Goulden, M.; Wofsy, S.; da Rocha, H.R.; de Camargo, P.B.; Crill, P.; Daube, B.C.; de Freitas, H.C.; *et al.* Carbon in Amazon forests: Unexpected seasonal fluxes and disturbance-induced losses. *Science* **2003**, *302*, 1554–1557.
40. Williams, C.A.; Albertson, J.D. Soil moisture controls on canopy-scale water and carbon fluxes in an African savanna. *Water Resour. Res.* **2004**, *40*, W09302.
41. Veenendaal, E.M.; Kolle, O.; Lloyd, J. Seasonal variation in energy fluxes and carbon dioxide exchange for a broad-leaved semi-arid savanna (Mopane woodland) in Southern Africa. *Glob. Chang. Biol.* **2004**, *10*, 318–328.
42. Lafleur, P.M.; Roulet, N.T.; Bubier, J.L.; Frolking, S.; Moore, T.R. Interannual variability in the peatland-atmosphere carbon dioxide exchange at an ombrotrophic bog. *Glob. Biogeochem. Cycles* **2003**, *17*, doi:10.1029/2002GB001983.
43. Giasson, M.-A.; Coursolle, C.; Margolis, H.A. Ecosystem-level CO_2 fluxes from a boreal cutover in eastern Canada before and after scarification. *Agric. For. Meteorol.* **2006**, *140*, 23–40.
44. Bergeron, O.; Margolis, H.A.; Black, T.A.; Coursolle, C.; Dunn, A.L.; Barr, A.G.; Wofsy, S.C. Comparison of carbon dioxide fluxes over three boreal black spruce forests in Canada. *Glob. Chang. Biol.* **2007**, *13*, 89–107.
45. Amiro, B.D.; Orchansky, A.L.; Barr, A.G.; Black, T.A.; Chambers, S.D.; Chapin, F.S., III; Goulden, M.L.; Litvak, M.; Liu, H.P.; McCaughey, J.H. The effect of post-fire stand age on the boreal forest energy balance. *Agric. For. Meteorol.* **2006**, *140*, 41–50.
46. Amiro, B.D. Paired-tower measurements of carbon and energy fluxes following disturbance in the boreal forest. *Glob. Chang. Biol.* **2001**, *7*, 253–268.
47. Rayment, M.B.; Jarvis, P.G. Seasonal gas exchange of black spruce using an automatic branch bag system. *Can. J. For. Res.* **1999**, *29*, 1528–1538.
48. Ammann, C.; Flechard, C.R.; Leifeld, J.; Neftel, A.; Fuhrer, J. The carbon budget of newly established temperate grassland depends on management intensity. *Agric. Ecosyst. Environ.* **2007**, *121*, 5–20.
49. Ammann, C.; Spirig, C.; Leifeld, J.; Neftel, A. Assessment of the nitrogen and carbon budget of two managed temperate grassland fields. *Agric. Ecosyst. Environ.* **2009**, *133*, 150–162.

50. Broquet, G.; Chevallier, F.; Bréon, F.-M.; Kadygrov, N.; Alemanno, M.; Apadula, F.; Hammer, S.; Haszpra, L.; Meinhardt, F.; Morguí, J.A. Regional inversion of CO_2 ecosystem fluxes from atmospheric measurements: Reliability of the uncertainty estimates. *Atmos. Chem. Phys.* **2013**, *13*, 9039–9056.
51. Anthoni, P.M.; Freibauer, A.; Kolle, O.; Schulze, E.-D. Winter wheat carbon exchange in Thuringia, Germany. *Agric. For. Meteorol.* **2004**, *121*, 55–67.
52. Owen, K.E.; Tenhunen, J.; Reichstein, M.; Wang, Q.; Falge, E.; Geyer, R.; Xiao, X.; Stoy, P.C.; Amman, C.; Arain, A.; *et al.* Linking flux network measurements to continental scale simulations: Ecosystem carbon dioxide exchange capacity under non-water-stressed conditions. *Glob. Chang. Biol.* **2007**, *13*, 734–760.
53. Knohl, A.; Schulze, E.-D.; Kolle, O.; Buchmann, N. Large carbon uptake by an unmanaged 250-year-old deciduous forest in Central Germany. *Agric. For. Meteorol.* **2003**, *118*, 151–167.
54. Don, A.; Rebmann, C.; Kolle, O.; Scherer-Lorenzen, M.; Schulze, E.-D. Impact of afforestation-associated management changes on the carbon balance of grassland. *Glob. Chang. Biol.* **2009**, *15*, 1990–2002.
55. Bernhofer, C.; Aubinet, M.; Clement, R.; Grelle, A.; Grünwald, T.; Ibrom, A.; Jarvis, P.; Rebmann, C.; Schulze, E.-D.; Tenhunen, J.D. Spruce forests (Norway and Sitka spruce, including Douglas fir): Carbon and water fluxes and balances, ecological and ecophysiological determinants. In *Fluxes of Carbon, Water and Energy of European Forests*; Springer: New York, NY, USA, 2003; pp. 99–123.
56. Anthoni, P.M.; Knohl, A.; Rebmann, C.; Freibauer, A.; Mund, M.; Ziegler, W.; Kolle, O.; Schulze, E.-D. Forest and agricultural land-use-dependent CO_2 exchange in Thuringia, Germany. *Glob. Chang. Biol.* **2004**, *10*, 2005–2019.
57. Kutsch, W.L.; Aubinet, M.; Buchmann, N.; Smith, P.; Osborne, B.; Eugster, W.; Wattenbach, M.; Schrumpf, M.; Schulze, E.D.; Tomelleri, E.; *et al.* The net biome production of full crop rotations in Europe. *Agric. Ecosyst. Environ.* **2010**, *139*, 336–345.
58. Casals, P.; Gimeno, C.; Carrara, A.; Lopez-Sangil, L.; Sanz, M. Soil CO_2 efflux and extractable organic carbon fractions under simulated precipitation events in a Mediterranean Dehesa. *Soil. Biol. Biochem.* **2009**, *41*, 1915–1922.
59. Gilmanov, T.G.; Soussana, J.F.; Aires, L.; Allard, V.; Ammann, C.; Balzarolo, M.; Barcza, Z.; Bernhofer, C.; Campbell, C.L.; Cernusca, A. Partitioning European grassland net ecosystem CO_2 exchange into gross primary productivity and ecosystem respiration using light response function analysis. *Agric. Ecosyst. Environ.* **2007**, *121*, 93–120.
60. Davi, H.; Dufrêne, E.; Francois, C.; Le Maire, G.; Loustau, D.; Bosc, A.; Rambal, S.; Granier, A.; Moors, E. Sensitivity of water and carbon fluxes to climate changes from 1960 to 2100 in European forest ecosystems. *Agric. For. Meteorol.* **2006**, *141*, 35–56.
61. Berbigier, P.; Bonnefond, J.-M.; Mellmann, P. CO_2 and water vapour fluxes for 2 years above Euroflux forest site. *Agric. For. Meteorol.* **2001**, *108*, 183–197.
62. Rambal, S.; Joffre, R.; Ourcival, J.-M. The growth respiration component in eddy CO_2 flux from a *Quercus ilex* Mediterranean forest. *Glob. Chang. Biol.* **2004**, *10*, 1460–1469.
63. Peichl, M.; Leahy, P.; Kiely, G. Six-year stable annual uptake of carbon dioxide in intensively managed humid temperate grassland. *Ecosystems* **2010**, *14*, 112–126.

64. Grünzweig, J.M.; Lin, T.; Rotenberg, E.; Schwartz, A.; Yakir, D. Carbon sequestration in arid-land forest. *Glob. Chang. Biol.* **2003**, *9*, 791–799.
65. Wohlfahrt, G.; Anderson-Dunn, M.; Bahn, M.; Balzarolo, M.; Berninger, F.; Campbell, C.; Carrara, A.; Cescatti, A.; Christensen, T.; Dore, S. Biotic, abiotic, and management controls on the net ecosystem CO_2 exchange of European mountain grassland ecosystems. *Ecosystems* **2008**, *11*, 1338–1351.
66. Reichstein, M.; Rey, A.; Freibauer, A.; Tenhunen, J.; Valentini, R.; Banza, J.; Casals, P.; Cheng, Y.; Grünzweig, J.M.; Irvine, J.; *et al.* Modeling temporal and large-Scale spatial variability of soil respiration from soil water availability, temperature and vegetation productivity indices. *Glob. Biogeochem. Cycles* **2003**, *17*, doi:10.1029/2003GB002035.
67. Skiba, U.; Drewer, J.; Tang, Y.S.; van Dijk, N.; Helfter, C.; Nemitz, E.; Famulari, D.; Cape, J.N.; Jones, S.K.; Twigg, M. Biosphere-atmosphere exchange of reactive nitrogen and greenhouse gases at the NitroEurope core flux measurement sites: Measurement strategy and first data sets. *Agric. Ecosyst. Environ.* **2009**, *133*, 139–149.
68. Cescatti, A.; Marcolla, B. Drag coefficient and turbulence intensity in conifer canopies. *Agric. For. Meteorol.* **2004**, *121*, 197–206.
69. Marcolla, B.; Cescatti, A.; Manca, G.; Zorer, R.; Cavagna, M.; Fiora, A.; Gianelle, D.; Rodeghiero, M.; Sottocornola, M.; Zampedri, R. Climatic controls and ecosystem responses drive the inter-annual variability of the net ecosystem exchange of an alpine meadow. *Agric. For. Meteorol.* **2011**, *151*, 1233–1243.
70. Marcolla, B.; Cescatti, A.; Montagnani, L.; Manca, G.; Kerschbaumer, G.; Minerbi, S. Importance of advection in the atmospheric CO_2 exchanges of an alpine forest. *Agric. For. Meteorol.* **2005**, *130*, 193–206.
71. Rey, A.; Pegoraro, E.; Tedeschi, V. Annual variation in soil respiration and its components in a coppice oak forest in Central Italy. *Glob. Chang. Biol.* **2002**, *8*, 851–866.
72. Chiesi, M.; Maselli, F.; Bindi, M.; Fibbi, L.; Cherubini, P.; Arlotta, E.; Tirone, G.; Matteucci, G.; Seufert, G. Modelling carbon budget of Mediterranean forests using ground and remote sensing measurements. *Agric. For. Meteorol.* **2005**, *135*, 22–34.
73. Jacobs, C.M.J.; Jacobs, A.F.G.; Bosveld, F.C.; Hendriks, D.M.D.; Hensen, A.; Kroon, P.S.; Moors, E.J.; Nol, L.; Schrier-Uijl, A.; Veenendaal, E.M. Variability of annual CO_2 exchange from Dutch grasslands. *Biogeosciences* **2007**, *4*, 803–816.
74. Moors, E.J.; Jacobs, C.; Jans, W.; Supit, I.; Kutsch, W.L.; Bernhofer, C.; Béziat, P.; Buchmann, N.; Carrara, A.; Ceschia, E. Variability in carbon exchange of European croplands. *Agric. Ecosyst. Environ.* **2010**, *139*, 325–335.
75. Dolman, A.J.; Moors, E.J.; Elbers, J.A. The carbon uptake of a mid latitude pine forest growing on sandy soil. *Agric. For. Meteorol.* **2002**, *111*, 157–170.
76. Chojnicki, B.H.; Urbaniak, M.; Józefczyk, D.; Augustin, J.; Olejnik, J. Measurements of gas and heat fluxes at Rzecin wetland. In *Wetlands: Monitoring, Modelling and Managemen*; Okrus, T., Maltby, E., Szatylowicz, J., Miroslaw-Swiatek, D., Kotowski, W., Eds.; Taylor & Francis: London, UK, 2007, 125–131.

77. Pereira, J.S.; Mateus, J.A.; Aires, L.M.; Pita, G.; Pio, C.; David, J.S.; Andrade, V.; Banza, J.; David, T.S.; Paço, T.A. Net ecosystem carbon exchange in three contrasting Mediterranean ecosystems-the effect of drought. *Biogeosciences* **2007**, *4*, 791–802.
78. Van der Molen, M.K.; van Huissteden, J.; Parmentier, F.J.W.; Petrescu, A.M.R.; Dolman, A.J.; Maximov, T.C.; Kononov, A.V; Karsanaev, S.V; Suzdalov, D.A. The growing season greenhouse gas balance of a continental tundra site in the Indigirka lowlands, NE Siberia. *Biogeosciences* **2007**, *4*, 985–1003.
79. Kurbatova, J.; Li, C.; Varlagin, A.; Xiao, X.; Vygodskaya, N. Modeling carbon dynamics in two adjacent spruce forests with different soil conditions in Russia. *Biogeosciences* **2008**, *5*, 969–980.
80. Kurbatova, J.; Arneth, A.; Vygodskaya, N.N.; Kolle, O.; Varlargin, A.V; Milyukova, I.M.; Tchebakova, N.M.; Schulze, E.; Lloyd, J. Comparative ecosystem-atmosphere exchange of energy and mass in a European Russian and a central Siberian bog I. Interseasonal and interannual variability of energy and latent heat fluxes during the snowfree period. *Tellus B* **2002**, *54*, 497–513.
81. Lagergren, F.; Eklundh, L.; Grelle, A.; Lundblad, M.; Mölder, M.; Lankreijer, H.; Lindroth, A. Net primary production and light use efficiency in a mixed coniferous forest in Sweden. *Plant Cell Environ.* **2005**, *28*, 412–423.
82. Gioli, B.; Miglietta, F.; de Martino, B.; Hutjes, R.W.A.; Dolman, A.J.; Lindroth, A.; Schumacher, M.; Sanz, M.J.; Manca, G.; Peressotti, A.; *et al.* Comparison between tower and aircraft-based eddy covariance fluxes in five European regions. *Agric. For. Meteorol.* **2004**, *127*, 1–16.
83. Herbst, M.; Rosier, P.T.W.; McNeil, D.D.; Harding, R.J.; Gowing, D.J. Seasonal variability of interception evaporation from the canopy of a mixed deciduous forest. *Agric. For. Meteorol.* **2008**, *148*, 1655–1667.
84. Fischer, M.L.; Billesbach, D.P.; Berry, J.A.; Riley, W.J.; Torn, M.S. Spatiotemporal variations in growing season exchanges of CO_2, H_2O, and sensible heat in agricultural fields of the southern Great Plains. *Earth Interact.* **2007**, *11*, 1–21.
85. Saito, M.; Maksyutov, S.; Hirata, R.; Richardson, A.D. An empirical model simulating diurnal and seasonal CO 2 flux for diverse vegetation types and climate conditions. *Biogeosciences* **2009**, *6*, 585–599.
86. Gilmanov, T.G.; Aires, L.; Barcza, Z.; Baron, V.S.; Belelli, L.; Beringer, J.; Billesbach, D.; Bonal, D.; Bradford, J.; Ceschia, E. Productivity, respiration, and light-response parameters of world grassland and agroecosystems derived from flux-tower measurements. *Rangel. Ecol. Manag.* **2010**, *63*, 16–39.
87. Meyers, T.P.; Hollinger, S.E. An assessment of storage terms in the surface energy balance of maize and soybean. *Agric. For. Meteorol.* **2004**, *125*, 105–115.
88. Oren, R.; Ellsworth, D.E.; Johnsen, K.H.; Phillips, N.; Ewers, B.E.; Maier, C.; Schäfer, K.V.R.; McCarthy, H.; Hendrey, G.; *et al.* Soil fertility limits carbon sequestration by forest-ecosystems in CO_2 enriched atmosphere. *Nature* **2001**, *411*, 469–472.
89. Gilmanov, T.G.; Tieszen, L.L.; Wylie, B.K.; Flanagan, L.B.; Frank, A.B.; Haferkamp, M.R.; Meyers, T.P.; Morgan, J.A. Integration of CO_2 flux and remotely-sensed data for primary production and ecosystem respiration analyses in the Northern Great Plains: Potential for quantitative spatial extrapolation. *Glob. Ecol. Biogeogr.* **2005**, *14*, 271–292.

90. Wilson, T.B.; Meyers, T.P. Determining vegetation indices from solar and photosynthetically active radiation fluxes. *Agric. For. Meteorol.* **2007**, *144*, 160–179.
91. Schmid, H.P.; Grimmond, C.S.B.; Cropley, F.; Offerle, B.; Su, H.B. Measurements of CO_2 and energy fluxes over a mixed hardwood forest in the mid-western United States. *Agric. For. Meteorol.* **2000**, *103*, 357–374.
92. Gu, L.; Meyers, T.; Pallardy, S.G.; Hanson, P.J.; Yang, B.; Heuer, M.; Hosman, K.P.; Riggs, J.S.; Sluss, D.; Wullschleger, S.D. Direct and indirect effects of atmospheric conditions and soil moisture on surface energy partitioning revealed by a prolonged drought at a temperate forest site. *J. Geophys. Res. Atmos.* **2006**, *111*, doi:10.1029/2006JD007161.
93. Cook, B.D.; Davis, K.J.; Wang, W.; Desai, A.; Berger, B.W.; Teclaw, R.M.; Martin, J.G.; Bolstad, P.V.; Bakwin, P.S.; Yi, C. Carbon exchange and venting anomalies in an upland deciduous forest in northern Wisconsin, USA. *Agric. For. Meteorol.* **2004**, *126*, 271–295.
94. Agarwal, D.A.; Humphrey, M.; Beekwilder, N.F.; Jackson, K.R.; Goode, M.M.; van Ingen, C. A data-centered collaboration portal to support global carbon-flux analysis. *Concurr. Comput. Pract. Exp.* **2010**, *22*, 2323–2334.
95. Juang, J.-Y.; Katul, G.G.; Porporato, A.; Stoy, P.C.; Siqueira, M.S.; Detto, M.; Kim, H.-S.; Oren, R. Eco-hydrological controls on summertime convective rainfall triggers. *Glob. Chang. Biol.* **2007**, *13*, 887–896.
96. Novick, K.; Brantley, S.; Miniat, C.F.; Walker, J.; Vose, J.M. Inferring the contribution of advection to total ecosystem scalar fluxes over a tall forest in complex terrain. *Agric. For. Meteorol.* **2014**, *185*, 1–13.
97. Kleidon, A. Nonequilibrium thermodynamics and maximum entropy production in the Earth system. *Naturwissenschaften* **2009**, *96*, 653–677.
98. Kleidon, A. Energy balance. In *Encyclopedia of Ecology*; Jørgensen, S.E., Fath, B.D., Eds.; Elsevier: Oxford, UK, 2008, Volume 2, pp. 1276–1289.
99. Luyssaert, S.; Jammet, M.; Stoy, P.; Estel, S.; Pongratz, J.; Ceschia, E.; Churkina, G.; Don, A.; Erb, K.; Ferlicoq, M.; *et al.* Land management and land-cover change have impacts of similar magnitude on surface temperature. *Nat. Clim. Chang.* **2014**, *4*, 389–393.
100. Luyssaert, S.; Schulze, E.D.; Borner, A.; Knohl, A.; Hessenmoller, D.; Law, B.E.; Ciais, P.; Grace, J. Old-growth forests as global carbon sinks. *Nature* **2008**, *455*, 213–215.
101. Hansen, M.C.; Potapov, P.V.; Moore, R.; Hancher, M.; Turubanova, S.A.; Tyukavina, A.; Thau, D.; Stehman, S.V.; Goetz, S.J.; Loveland, T.R.; *et al.* High-Resolution Global Maps of 21st-Century Forest Cover Change. *Science* **2013**, *342*, 850–853.
102. De Frenne, P.; Rodríguez-Sánchez, F.; Coomes, D.A.; Baeten, L.; Verstraeten, G.; Vellend, M.; Bernhardt-Römermann, M.; Brown, C.D.; Brunet, J.; Cornelis, J. Microclimate moderates plant responses to macroclimate warming. *Proc. Natl. Acad. Sci. USA* **2013**, *110*, 18561–18565.
103. Norris, C.; Hobson, P.; Ibisch, P. Microclimate and vegetation function as indicators of forest thermodynamic efficiency. *J. Appl. Ecol.* **2011**, *49*, 562–570.